Coupling stabilizers open K_V1-type potassium channels

Malin Silverå Ejneby[a], Björn Wallner[b], and Fredrik Elinder[a,1]

[a]Department of Biomedical and Clinical Sciences, Linköping University, SE-581 85 Linköping, Sweden; and [b]Department of Physics, Chemistry, and Biology, Linköping University, SE-581 83 Linköping, Sweden

Edited by Ehud Y. Isacoff, University of California, Berkeley, CA, and approved September 15, 2020 (received for review April 24, 2020)

The opening and closing of voltage-gated ion channels are regulated by voltage sensors coupled to a gate that controls the ion flux across the cellular membrane. Modulation of any part of gating constitutes an entry point for pharmacologically regulating channel function. Here, we report on the discovery of a large family of warfarin-like compounds that open the two voltage-gated type 1 potassium (K_V1) channels $K_V1.5$ and Shaker, but not the related K_V2-, K_V4-, or K_V7-type channels. These negatively charged compounds bind in the open state to positively charged arginines and lysines between the intracellular ends of the voltage-sensor domains and the pore domain. This mechanism of action resembles that of endogenous channel-opening lipids and opens up an avenue for the development of ion-channel modulators.

potassium-channel openers | VSD-to-pore coupling | K_V1 channel

Voltage-gated ion channels are transmembrane pores located in the cellular membrane of all cells, allowing charged ions to cross the membrane to alter cellular function (1). They are sensitive to alterations in the transmembrane voltage; the movement of intrinsic voltage sensors is linked to the channel gate (Fig. 1*A*). Opening and closing of such channels initiate and terminate nervous or cardiac impulses, leading to motions, sensations, and thoughts. Thus, these channels are obvious targets for endogenous and pharmaceutical compounds to control diseases such as epilepsy, cardiac arrythmia, and pain (2). However, the principles for how specific channels are targeted and modulated by small-molecule compounds are largely unknown. For example, while ion-channel inhibitors, such as local anesthetics, have been studied in detail (3–7), less information is available for ion-channel activators; if the molecular mechanism of action is known at all, activators have been found to act on either the voltage-sensor domain (VSD) (1 in Fig. 1*A*) (8–12) or the pore domain (2 in Fig. 1*A*) (13–15). Here, we describe the discovery of a large family of warfarin-like compounds that selectively activate voltage-gated type 1 potassium (K_V1) channels by binding to two pockets formed between the VSDs and the pore domain (3 in Fig. 1*A*). This is an example of a small-molecule ion-channel activator stabilizing the VSD–pore coupling in the open state.

Results

Exploration of 10,096 Compounds in a High-Throughput Screen. To search for specific K_V-channel activators and for common molecular motifs, we developed high-throughput methodology to measure the effect of an array of compounds on the Shaker K_V channel (*Materials and Methods*). In total, we obtained data from 10,096 unique compounds at a concentration of 10 μM; 822 compounds were significant activators (blue dots in Fig. 1*B*), 6,892 compounds had no significant effect (black dots), and 2,382 compounds inhibited the channel significantly (red dots). Not surprisingly, the group of K_V-channel activators contained many types of compounds, but we identified a large family (247 compounds) (*SI Appendix*, Table S1) of potent channel activators with a well-defined tautomer motif (Fig. 1*C*).

The Tautomeric Channel-Opening Motif. Tautomeric compounds are constitutional isomers that readily interconvert, in many cases by relocating a proton (Fig. 1*C*, isom). Furthermore, the motif can be deprotonated and consequently, negatively charged (Fig. 1*C*, prot). We will refer to the compounds as C, N, or O compounds depending on the signature atom in the central ring (Fig. 1*C*); 3 of the compounds are C compounds, 209 are N compounds, and 35 are O compounds. Some of the O compounds, also called 4-hydroxycoumarines, inhibit vitamin K epoxide reductase and are used as vitamin K antagonist anticoagulants (16) (e.g., warfarin), but to our knowledge, none of the compounds have ever been reported to open ion channels. In total, 108 of the tautomer compounds were significant activators, 119 had no significant effect, and 20 were significant (but weak) inhibitors (*SI Appendix*, Table S1). The probability to find tautomer compounds among all tested compounds increased with larger opening effects (Fig. 1*D*): among the 157 activators that increase the current by >50%, 59 (38%) belong to the tautomer family, and 16 of the 23 most potent activators belong to this family.

The best tautomer activators share several molecular characteristics (*SI Appendix*, Fig. S1). 1) The molecular weight is 300 to 450 Da, 2) the octanol/water partition coefficient (log *P*) value is four to six, and 3) the acidic dissociation constant (pK_a) value is <7.4. Thus, the strong activators are likely to be relatively lipophilic and mostly negatively charged at neutral pH. To further explore if the charge of the tautomer motif is important for channel opening, we searched for motifs similar to the tautomer motifs but expected to be uncharged, with two double-bonded oxygens (=O/=O) instead of the tautomer motif (−OH/=O). In total, we identified 739 such compounds, but they were not overrepresented among the activators (Fig. 1*E*), suggesting that this uncharged motif does not affect gating. Taken together, these data suggest that the charged tautomer motif constitutes a robust channel-opening scaffold, probably binding to a common pocket, and that the specific side chains (R1 to R4) fine tune the channel-opening properties.

Role of Side Chains of the Tautomer Compounds. One intriguing aspect of the tautomer motif is its simple structure; 149 of the

Significance

Voltage-gated ion channels are transmembrane pores responsible for the generation and transmission of nervous impulses. They are also obvious targets for pharmaceutical drugs against neurological diseases. A challenge is to develop compounds that target a specific ion channel. Here, we report on the discovery of a large family of compounds that specifically open one subfamily of potassium channels. These compounds act on the linker between the channel's voltage sensor and gate to keep the channel open. These findings open up an avenue for the development of ion-channel modulators.

Author contributions: M.S.E., B.W., and F.E. designed research; M.S.E., B.W., and F.E. performed research; F.E. contributed new reagents/analytic tools; M.S.E., B.W., and F.E. analyzed data; and M.S.E., B.W., and F.E. wrote the paper.

The authors declare no competing interest.

This article is a PNAS Direct Submission.

[1]To whom correspondence may be addressed. Email: fredrik.elinder@liu.se.

This article contains supporting information online at https://www.pnas.org/lookup/suppl/doi:10.1073/pnas.2007965117/-/DCSupplemental.

First published October 13, 2020.

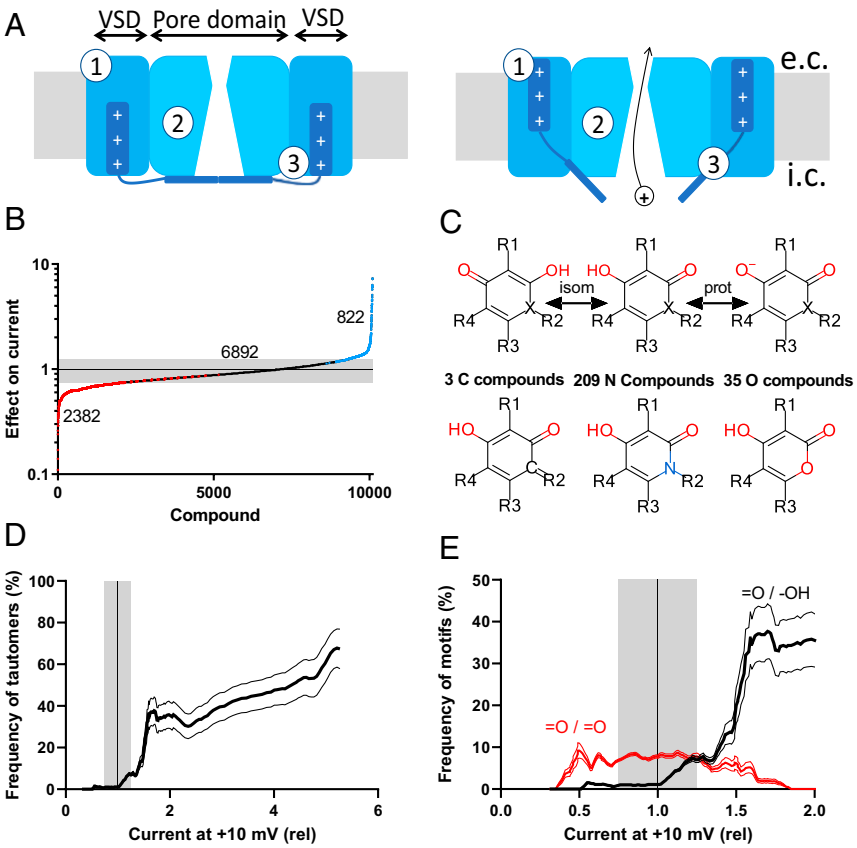

Fig. 1. A high-throughput screen identified a large family of K_V-channel activators. (*A*) Cartoons of a closed (*Left*) ion channel and an open (*Right*) ion channel. Numbers 1 and 2 denote previously identified binding sites for ion-channel modulators. Number 3 denotes the binding site identified in the present investigation. e.c., extracellular side of the membrane; i.c., intracellular side. (*B*) Effect on the current (compound/control) at the end of a 150-ms pulse to +10 mV, from a holding voltage of −80 mV. Blue data points denote 822 significant activators (*Materials and Methods* discusses significance determination), red data points denote 2,382 inhibitors, and black data points denote 6,892 noneffective. The gray field represents nonsignificant effects for single experiments. (*C*) Structures of the central tautomer ring, important transitions, and numbers of C, N, and O compounds. isom, isomerization step; prot, (de-)protonation step; R1 to R4, side chains of different types. (*D*) Frequency of the tautomer compounds among all 10,096 tested compounds vs. effect on the current (*Materials and Methods* shows the calculation). Thin lines represent 95% CIs. (*E*) Same as *D* but data for compounds with double-bonded oxygens have been included.

247 compounds have four separate, nonconnected side chains (R1, R2, R3, and R4) (Fig. 1*C*), while 98 compounds have two or three side chains connected in different types of aromatic and nonaromatic ring structures. The most potent channel-opening compounds have rather diverse shapes (Fig. 2). The most efficacious channel activator of all investigated compounds is one of the C compounds (Fig. 2 *A*, *a*). Also, among the O compounds (Fig. 2 *A*, *b* and *c*) and the N compounds (Fig. 2 *A*, *d*–*g*), there are many potent channel activators. The C and O compounds in most cases have one side chain (R1) and one ring structure (Fig. 2 *A*, *a*–*c*). The N compounds, which constitute 85% (209 of 247) of all tautomer compounds, have either four distinct side chains (Fig. 2 *A*, *d* and *e*) or side chains in combinations with ring structures (Fig. 2 *A*, *f* and *g*). It is furthermore apparent that subtle changes of the structure can render the compounds inactive with respect to their channel-opening capacity (Fig. 2 *A*, *c*, *e*, and *g*). For instance, polar or short side chains at R1 result in compounds that lack most, if not all, channel-opening capacity (Fig. 2 *A*, *e* and *g*). Warfarin (#138) (*SI Appendix*, Table S1), found among the O compounds, had a small but significant channel-opening effect (1.18 ± 0.05, $n = 7$, $P = 0.0112$) (Fig. 2 *A*, *c*). However, it should be pointed out that low activity does not necessarily reflect a low affinity of efficacy of the compound bound to the site of action but might reflect a reduced penetration to the site of action.

To obtain in-depth information regarding which side chains of the compounds are important for channel opening and to resolve the size and properties of the binding pocket, we performed an analysis based on two assumptions (*Materials and Methods*): 1) the side chains contribute to the channel-opening effect independent of each other, and 2) the channel-opening effect depends on the product of the effect of the individual side chains. We determined the best solution, by a least-square method, of a large system of Eq. **1** (*Materials and Methods*, Fig. 2*B*, and *SI Appendix*, Fig. S2 and Table S1). It is not possible to determine the relative roles of side chains at different locations (i.e., the role of a side chain R1 compared with R2), but one can compare the roles of different side chains at the same location (Fig. 2*B*). For R1, the most effective side chain to open the channel was a sulfur-connected phenyl group (with zero to three chlorines). The least effective were polar (sulfone) or short side chains (iodine, isopropyl). For R2, an aromatic ring (with or without chlorines or methyl groups attached) connected directly to the nitrogen in the central ring had clear channel-opening effects, while short hydrocarbon chains had only small effects, if any. For R3, the most effective side chain was a methyl group, while aromatic rings or branched hydrocarbons had no or only small

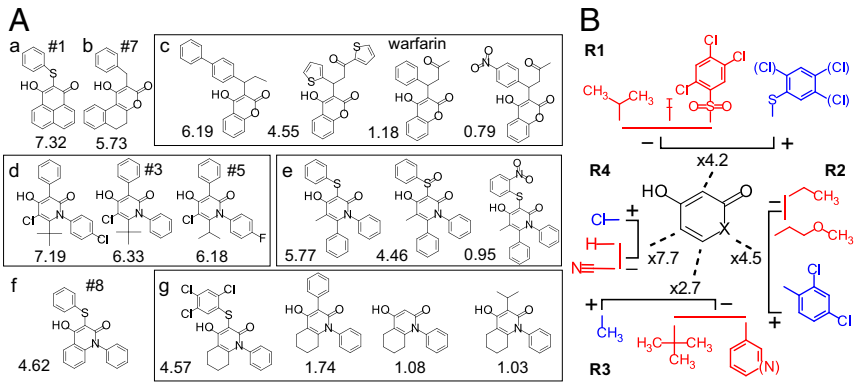

Fig. 2. Structures of tautomer compounds. (*A*) Selection of structures in different clusters (*a*–*g*). The numbers below the structures are the x-fold channel-opening effect at +10 mV. Compounds #1, #3, #5, #7, and #8 and warfarin (#138) were selected for more detailed investigations. (*B*) Relative roles of some side chains for the channel-opening effect. Blue denotes the most potent side chains, and red denotes the least potent. Factors (xX) denote the relative effects between the blue and red clusters for each side chain (*Materials and Methods* shows the calculation).

effects. For R4, the most effective side chain was a chlorine, while hydrogen or polar (nitrile) side chains had no apparent effect. Overall, strongly polar side chains reduced the channel-opening effects. For R1 and R2, larger (aromatic) side chains opened the channel, while for R3 and R4, short hydrocarbon or chlorine chains opened the channel.

The Tautomeric Compounds Open the Wild-Type Shaker K_V Channel. To explore the molecular mechanisms of action of the tautomer compounds, we selected five compounds of diverse structures and very strong channel-opening effects (compounds #1, #3, #5, #7, and #8 in Fig. 2*A* and *SI Appendix*, Table S1) and the less effective warfarin (compound #138 in Fig. 2 *A*, *c* and *SI Appendix*, Table S1). We explored the effect on the wild-type (WT) Shaker K_V channel and the 3R Shaker K_V mutant (M356R/A359R; used in the screen) expressed in *Xenopus laevis* oocytes. The onset (*SI Appendix*, Fig. S3) and the offset of the effects were complete within a minute. There was no difference in concentration dependence ($c_{1/2}$) between the two channels (*SI Appendix*, Fig. S4), and the maximum shift (ΔV_{MAX}) was only modestly affected, suggesting that the 3R motif had only minor effects and justifying the use of the WT in the following analysis; 100 μM #1 had a massive opening effect on the WT Shaker K_V channel (Fig. 3*A*) and shifted the conductance vs. voltage, $G(V)$, curve along the voltage axis by −24.2 ± 0.3 mV ($n = 5$) (Fig. 3*B*). All compounds opened the channel by shifting the $G(V)$ curve along the voltage axis, #1 being most effective and warfarin being least effective (Fig. 3*C*). The maximum shift was not apparently compound dependent. Compound #1 did not affect the opening kinetics of the WT Shaker K_V channel but slowed down the closing kinetics (*SI Appendix*, Fig. S5), suggesting that the compound stabilizes the channel in an open state with no effect on the closed state.

A Tentative Intracellular Binding Site. The analysis above suggested that the negatively charged form of the tautomers is the active one. To directly alter the charge of the tautomers, we altered the pH; at high pH, the tautomers are expected to be negatively charged and at low pH, uncharged. Surprisingly, all explored compounds (at 30 μM) showed an increased effect at lower pH (Fig. 3*D*) (i.e., when the compounds were expected to be uncharged). This contradicts the before-mentioned suggestion that uncharged compounds are inactive. We hypothesize that the neutral variant of the compound is needed to reach the binding site, while the negatively charged variant is needed to exert a functional effect when bound to the site of action. It is possible that the neutral form of the compound is necessary to cross the cell membrane, and well inside the cell, the compound becomes (partly) negatively charged and in this form, binds to and activates the channel. In line with this suggestion, the on rate of the effect after application of the substance is faster at low pH, when the compound is expected to be neutral and able to pass the membrane (*SI Appendix*, Fig. S3). This is similar to the membrane-passing strategy used by local anesthetics (3).

Selective Opening of K_V1-Type Potassium Channels. To search for possible intracellular sites, we first explored the effects on other K_V channels; 100 μM compound #1 shifted the $G(V)$ of the WT Shaker K_V channel by –24.2 ± 0.3 mV at pH 7.4 (Fig. 3 *B* and *F* and *SI Appendix*, Fig. S6 *A* and *F*). However, no shift of the $G(V)$ curve was found for human (h)K_V2.1 [but a voltage-independent reduction of the $G(V)$], hK_V4.1, or hK_V7.2/7.3, while 100 μM #1 shifted the $G(V)$ curve of hK_V1.5 by –14.5 ± 1.1 mV (Fig. 3 *E* and *F* and *SI Appendix*, Fig. S6 *B*–*F*). For hK_V1.5, ΔV_{MAX} was –16.5 ± 2.9 mV, and $c_{1/2}$ was 10.4 ± 2.9 μM ($n = 3$ to 5) (Fig. 3*G*). Thus, the channel's voltage dependence for the K_V1-type Shaker K_V and K_V1.5 channels was clearly sensitive to the tautomer compounds, while channels from the subfamilies K_V2, K_V4, and K_V7 were not. This lack of effect was not unique for compound #1. None of the compounds #1, #3, #5, #7, and #8 shifted the $G(V)$ of K_V4.1 (*SI Appendix*, Fig. S7).

Binding to the Intracellular S4–S5 Linker: Molecular Docking. To search for possible binding sites, we compared the amino acid sequences of the explored K_V channels on the intracellular side, in the vicinity on the transmembrane segments. There are three positions where the residues are positively charged in the K_V1-type channels and uncharged or negatively charged in the K_V2.1, K_V4.1, K_V7.2, and K_V7.3 (*SI Appendix*, Fig. S6*G*); two residues are located close to or in the S4–S5 linker (connecting the VSD and the pore domain; K380 and R387 in the Shaker K_V channel), and one is in the intracellular end of S6 (R487). To test for binding poses close to these three residues, we docked the 15 most potent compounds to an homology model of the Shaker K_V channel (17). All compounds found stable binding poses to the channel (Fig. 4*A* and *SI Appendix*, Fig. S8). Fourteen of the 15 compounds preferentially bound to one of two sites (sites A and B) (Fig. 4 *B* and *C* and *SI Appendix*, Fig. S8). Eight of the compounds mainly bound to a pocket surrounded by residues D310, V311, and M312 at the intracellular end of S3 and residues Q383, G386, and R387 in the S4–S5 linker (site A) (Fig. 4 *B* and *C*). Six compounds mainly bound to a pocket surrounded by

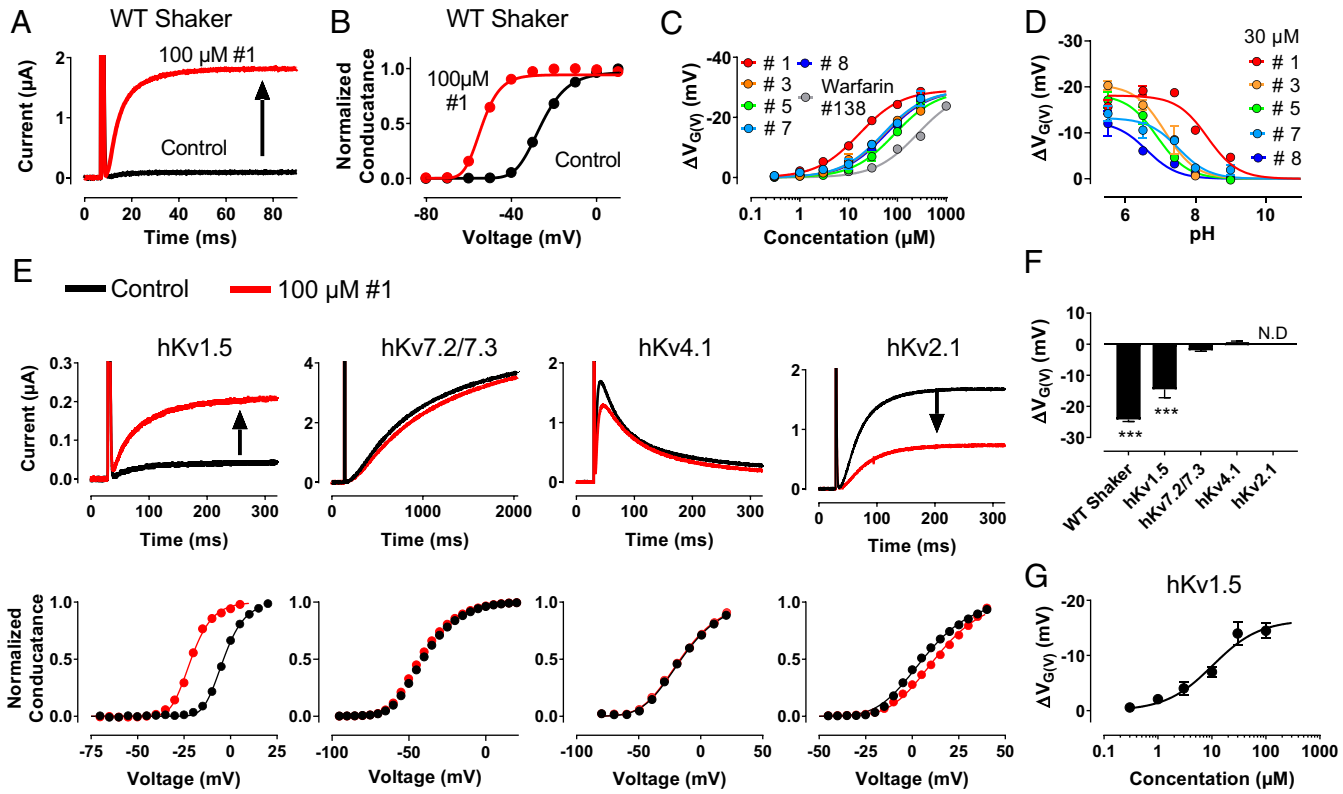

Fig. 3. The tautomer compounds open K_V channels. Molecular structures of compounds #1, #3, #5, #7, and #8 and warfarin are shown in Fig. 2*A*. For all experiments and data, expression system is in *Xenopus* oocytes, holding voltage = −80 mV, pH is 7.4 (if not otherwise stated), mean ± SEM, and *n* is the number of experiments for each data point. (*A*) Effect of compound #1 on WT Shaker K_V at −40 mV. (*B*) *G*(*V*) curve for the cell in *A*. (*C*) Concentration–response curves for WT Shaker K_V. $n = 3$. $\Delta V_{MAX} = -29.1$ mV (shared for all compounds). $c_{1/2}$: 16.6 ± 1.5 μM (#1), 53.5 ± 5.1 μM (#3), 88.6 ± 8.4 μM (#5), 51.1 ± 4.9 μM (#7), 58.7 ± 5.6 μM (#8), and 259 ± 25 (warfarin, #138). (*D*) pH dependence for *G(V)* shifts for 30 μM compounds on WT Shaker K_V. $n = 3$ to 5. pK_a/ΔV_{MAX}: 8.3/−18.1 mV (#1), 7.1/−20.5 mV (#3), 6.9/−18.4 mV (#5), 7.5/−13.3 mV (#7), and 6.6/−12.5 mV (#8). (*E*) Effect of 100 μM compound #1 at −40 mV ($hK_V1.5$, $hK_V7.2/7.3$) or 0 mV ($hK_V4.1$/hK_V 2.1; *Upper*) and corresponding *G*(*V*) curves (*Lower*) for the denoted channels. (*F*) Summary of *G*(*V*) shift as recorded in *E*. $n = 3$ to 6. N.D. means that the shift could not be reliably determined, but it is clear that there were no negative shifts. ***$P < 0.001$. (*G*) Concentration–response curves for $hK_V1.5$, compound #1. $c_{1/2} = 10.4 \pm 2.9$ μM, $\Delta V_{MAX} = -16.5 \pm 2.9$. $n = 3$ to 5.

residues S379, K380, and G381 at the intracellular end of S4 and R394, G397, and L398 at the intracellular end of S5 of an adjacent subunit (site B) (Fig. 4 *B* and *C*). Also, A489, at the intracellular end of S6, is close to site B, but we do not know if this is involved in a native channel, which has an extended S6. The last compound (#10) fits equally well into both pockets (*SI Appendix*, Fig. S8).

There are some structural features of the site A and site B tautomer compounds. The most obvious is that all O compounds bind to site B. However, two pairs of N compounds with only minor structural differences bind to different sites, suggesting that the two pockets probably are very similar and probably can host both types of molecules, and possibly both sites can be occupied simultaneously by two discrete molecules. K380 is located in the site B pocket, and R387 is in site A. In contrast, R487 is not part of any of the pockets. In addition, the positively charged residue R394 at the intracellular end of S5, which is not unique for Kv1-type channels, is located in the site B pocket. The suggested binding sites have clear functional implications. Binding of the compound to site A (Fig. 4*C*) keeps the S4–S5 linker in a horizontal position, which is associated with an open channel (18). Binding to site B (Fig. 4*C*) pulls S5 and possibly also S6 toward S4, leading to the opening of the channel. Recently, the first closed, resting-state model of a voltage-gated ion channel (a bacterial Na channel) was described (19). This closed-state structure makes it possible to test our proposed opening mechanisms. In the closed state, both binding sites A and B are clearly disrupted (judged as a substantial separation between the important residues), suggesting that binding to sites A and B keeps the channel in an open state (Fig. 4*D*).

Binding to the Intracellular S4–S5 Linker: Experiments. Finally, to functionally test the hypothesis that the tautomer compounds bind to the site A or B, we neutralized both K380 and R387, in an attempt to disrupt binding to any of the two sites. The double mutation K380Q/R387Q completely removed the *G*(*V*)-shifting effect of compound #1 at 10 μM (Fig. 4*E*) and increased $c_{1/2}$ from 16.3 ± 2.4 to 191 ± 33 μM ($n = 3$ to 4) (Fig. 4*F*). One possibility for the remaining low-affinity activity is binding to unrelated sites from the extracellular side. To test this, we performed experiments at pH 5.5 where the compound is expected to be uncharged in the extracellular solution. pH 5.5 completely removed the *G*(*V*) shift at 100 μM (Fig. 4*F*), while the effect on WT at pH 5.5 was not different from pH 7.4 (*SI Appendix*, Fig. S9*A*). Also, the single mutation R387Q significantly increased #1 $c_{1/2}$ (to 36.9 ± 7.1 μM; $n = 3$ to 4) (*SI Appendix*, Fig. S9*B*), supporting the idea that site A acting compounds partly depend on R387. The double mutation K380Q/R387Q also clearly reduced the effects for the site B compound #7 and the site A compound #5 (*SI Appendix*, Fig. S9 *C* and *D*). The single mutation R387Q, which only should affect site A, strikingly did not affect the site B compound #7 at all (*SI Appendix*, Fig. S9*C*). Thus, disruption of the putative binding sites by mutation clearly supports the modeling data.

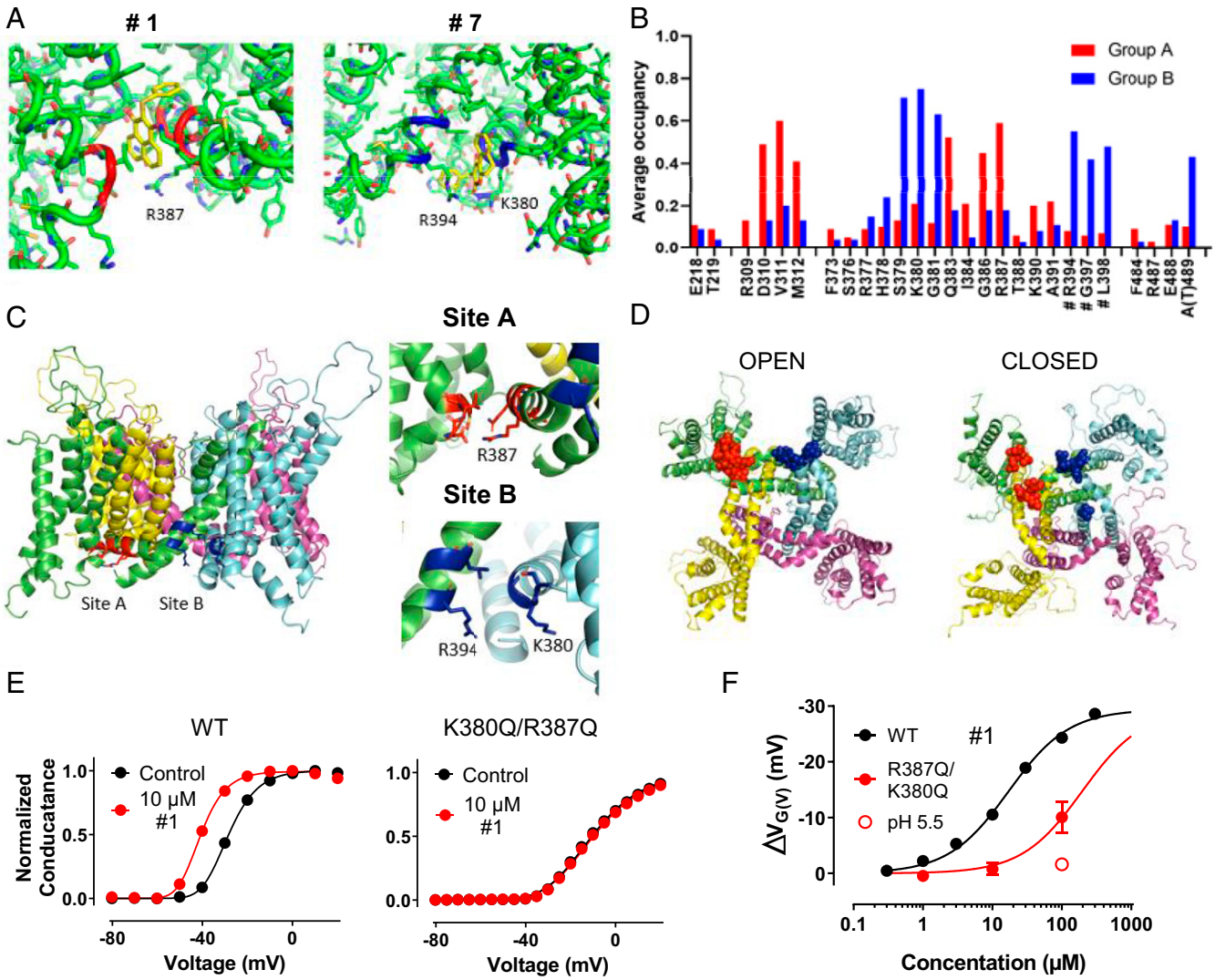

Fig. 4. Druggable binding sites. (*A*) Best binding poses of compounds #1 and #7. Compound #1 prefers binding pose/site A (red). Compound #7 prefers binding pose/site B (blue). (*B*) Mean of average occupancy for site A compounds (red) and site B compounds (blue) (*Materials and Methods* shows the calculation). (*C*) Binding pockets for site A compounds (red residues 310 to 312, 383, 386, and 387) and site B compounds (blue residues 379 to 381, 394, 397, and 398). Different colors are for different subunits. (*D*) Homologous residues from *C* in open and closed structures (17, 19). (*E*) *G*(*V*) curves for WT and K380Q/R387Q Shaker K_V, with and without 10 μM compound #1. (*F*) Concentration–response curves for compound #1 as denoted. $c_{1/2}$ (WT) = 17.1 ± 2.5 μM, $c_{1/2}$ (R380Q/R387Q) = 196 ± 32 μM, ΔV_{MAX} (shared value) = −29.4 ± 1.1 mV. All data are mean ± SEM; n = 3 to 4. pH is 7.4 except for the open symbol, where pH is 5.5 for K380Q/R387Q.

Discussion

We have described the finding of a large family of compounds that share a common tautomer motif and that selectively open the gate of K_V1-type channels (Shaker K_V and hK_V1.5). Previously reported gating modifiers of voltage-gated ion channels solely bind to the VSD (6, 8–12, 20) or to the pore domain (13–15, 21). In contrast, the tautomeric compounds explored herein act in direct contact with the voltage sensor to pore coupling. Even though we have not specifically explored the functional coupling, the important residues are clearly located in the anatomical coupling between the VSD and the pore domain. Intriguingly, the tautomer binding site A in the K_V1 channels overlaps with the binding site for the negatively charged lipid phosphatidylinositol 4,5-bisphosphate of K_V7.1 (22), where it is required to increase the coupling between the gate and the voltage sensor (23). This binding site is also close to the bindings site of capsaicin in the essentially voltage-independent transient receptor potential cation channel subfamily V member 1 (TRPV1) channel (24). Thus, we envision that the findings described here can be used to develop pharmaceutical compounds that stabilize the coupling between the VSD and the pore domain in a desired state.

Materials and Methods

Detailed materials and methods are described in *SI Appendix*.

Studied K_V Channels and Molecular Biology. The following channels were used in this study: the *Drosophila* Shaker H4 channel (25) with removed N-type inactivation (ShH4IR) (25); the 3R Shaker K_V-channel mutant (i.e., M356R and A359R) (26); and human K_V1.5, K_V2.1, K_V4.1, K_V7.2, and K_V7.3. K_V7.2/7.3 was injected in a 1:1 ratio as described previously (27).

High-Throughput Screen. The high-throughput screen has been described elsewhere (refs. 9 and 28 and references therein).

Calculated Chemical Properties. Marvin and JChem for Office (ChemAxon) were used for drawing chemical structures and calculations as previously described (9, 29).

Calculation of Side-Chain Effects. To quantitatively analyze the role of the side chains, we solved a system of 121 equations on the empirically derived form

$$P_{R1x} \times P_{R2x} \times P_{R3x} \times P_{R4x} = P_{totx}, \quad [1]$$

where P is the effect of each individual side chain (R1 to R4) on channel opening for compound x and P_{totx} is the total predicted effect of compound x.

Manual Two-Electrode Voltage Clamp Recordings. All animal experiments were approved by Linköping's local animal care and use committee. Surgery on *X. laevis* frogs, isolation of oocytes, and storage of oocytes have been described in detail previously (30, 31). K^+ currents were measured with the two-electrode voltage clamp technique as described previously (29). The conductance, $G(V)$, was calculated as

$$G(V) = I_K/(V - V_K), \quad [2]$$

where I_K is the average steady-state current, V is the absolute membrane voltage, and V_K is the reversal potential (set to –80 mV). The data were fitted to

$$G(V) = A/\left(1 + \exp((V_{½} - V)/s)\right)^n, \quad [3]$$

where A is the amplitude, $V_{1/2}$ is the midpoint (if $n = 1$), s is the slope, and n is an exponent. $G(V)$ shifts were measured at the foot of the $G(V)$ curve as described previously (11, 32). Concentration dependence for the compounds was quantified by

$$\Delta V = V_{MAX}/\left(1 + c_{½}/c\right), \quad [4]$$

where ΔV is the voltage shift, V_{MAX} is the amplitude, c is the concentration, and $c_{1/2}$ is the concentration at which half-maximum response occurs. The time constant τ for opening and closing kinetics was calculated from a single exponential function:

$$I(t) = A \exp(-t/\tau) + C, \quad [5]$$

where t is the time, A is the amplitude, τ is the time constants, and C is a constant.

Molecular Docking. The 15 most potent compounds from the high-throughput screen (*SI Appendix*, Table S1) were docked against a model of all chains in the tetrameric Shaker K_V channel.

Statistical Analysis. Mean values are expressed as mean ± SEM. A two-tailed, one-sample t test, in which the mean value was compared with a hypothetical value of zero, was used to analyze $G(V)$ shifts. To compare two different conditions, a Student's t test was used. $P < 0.05$ was considered significant for all statistical tests: $*P < 0.05$, $**P < 0.01$, and $***P < 0.001$.

Data Availability. All study data are included in the article and *SI Appendix*.

ACKNOWLEDGMENTS. We thank Per-Eric Lund for performing the high-throughput experiments; Gunnar Nordvall for chemistry advice and compound selection; Anders B Eriksson, SciLifeLab, for help with compound handling; Andreas Nolting for construction of the cell line; and William Lövfors and Gunnar Cedersund for assistance with Matlab calculations. We also thank Stefan Thor, Peter Larsson, Sara Liin, and Antonios Pantazis for comments on the manuscript. We thank the Chemical Biology Consortium Sweden (CBCS) at Science for Life Laboratory for providing the chemical libraries tested in the screen. The NIH Clinical Collection was provided through the NIH Molecular Libraries Roadmap Initiative. The Laboratories for Chemical Biology Karolinska Institutet primary screening set was provided by CBCS. Part of this work was assisted by Karolinska High Throughput Center, a core facility at Karolinska Institutet with affiliation to Science for Life Laboratory (https://www.scilifelab.se/facilities/khtc/). The computations were performed on resources provided by the Swedish National Infrastructure for Computing at the National Supercomputer Centre (https://www.nsc.liu.se/). This work was supported by Swedish Research Council Grant 2016-02615, Swedish Heart-Lung Foundation Grant 20150672, and Swedish Brain Foundation Grant 2016-0326.

1. B. Hille, *Ion Channels of Excitable Membranes*, (Sinauer Associates Inc., 2001).
2. F. M. Ashcroft, *Ion Channels and Disease*, (Academic Press, 1999).
3. B. Hille, Local anesthetics: Hydrophilic and hydrophobic pathways for the drug-receptor reaction. *J. Gen. Physiol.* **69**, 497–515 (1977).
4. D. S. Ragsdale, J. C. McPhee, T. Scheuer, W. A. Catterall, Molecular determinants of state-dependent block of Na+ channels by local anesthetics. *Science* **265**, 1724–1728 (1994).
5. M. Zhou, J. H. Morais-Cabral, S. Mann, R. MacKinnon, Potassium channel receptor site for the inactivation gate and quaternary amine inhibitors. *Nature* **411**, 657–661 (2001).
6. S. Ahuja *et al.*, Structural basis of Nav1.7 inhibition by an isoform-selective small-molecule antagonist. *Science* **350**, aac5464 (2015).
7. D. Jiang *et al.*, Structure of the cardiac sodium channel. *Cell* **180**, 122–134.e10 (2020).
8. A. Peretz *et al.*, Targeting the voltage sensor of Kv7.2 voltage-gated K+ channels with a new gating-modifier. *Proc. Natl. Acad. Sci. U.S.A.* **107**, 15637–15642 (2010).
9. S. I. Liin *et al.*, Biaryl sulfonamide motifs up- or down-regulate ion channel activity by activating voltage sensors. *J. Gen. Physiol.* **150**, 1215–1230 (2018).
10. S. I. Börjesson, F. Elinder, An electrostatic potassium channel opener targeting the final voltage sensor transition. *J. Gen. Physiol.* **137**, 563–577 (2011).
11. N. E. Ottosson *et al.*, A drug pocket at the lipid bilayer-potassium channel interface. *Sci. Adv.* **3**, e1701099 (2017).
12. P. Li *et al.*, The gating charge pathway of an epilepsy-associated potassium channel accommodates chemical ligands. *Cell Res.* **23**, 1106–1118 (2013).
13. T. V. Wuttke, G. Seebohm, S. Bail, S. Maljevic, H. Lerche, The new anticonvulsant retigabine favors voltage-dependent opening of the Kv7.2 (KCNQ2) channel by binding to its activation gate. *Mol. Pharmacol.* **67**, 1009–1017 (2005).
14. M. Schewe *et al.*, A pharmacological master key mechanism that unlocks the selectivity filter gate in K^+ channels. *Science* **363**, 875–880 (2019).
15. Q. Xiong, H. Sun, M. Li, Zinc pyrithione-mediated activation of voltage-gated KCNQ potassium channels rescues epileptogenic mutants. *Nat. Chem. Biol.* **3**, 287–296 (2007).
16. D. S. Whitlon, J. A. Sadowski, J. W. Suttie, Mechanism of coumarin action: Significance of vitamin K epoxide reductase inhibition. *Biochemistry* **17**, 1371–1377 (1978).
17. U. Henrion *et al.*, Tracking a complete voltage-sensor cycle with metal-ion bridges. *Proc. Natl. Acad. Sci. U.S.A.* **109**, 8552–8557 (2012).
18. S. B. Long, X. Tao, E. B. Campbell, R. MacKinnon, Atomic structure of a voltage-dependent K+ channel in a lipid membrane-like environment. *Nature* **450**, 376–382 (2007).
19. G. Wisedchaisri *et al.*, Resting-state structure and gating mechanism of a voltage-gated sodium channel. *Cell* **178**, 993–1003.e12 (2019).
20. K. J. Swartz, R. MacKinnon, Hanatoxin modifies the gating of a voltage-dependent K+ channel through multiple binding sites. *Neuron* **18**, 665–673 (1997).
21. I. Kopljar *et al.*, The ladder-shaped polyether toxin gambierol anchors the gating machinery of Kv3.1 channels in the resting state. *J. Gen. Physiol.* **141**, 359–369 (2013).
22. J. Sun, R. MacKinnon, Structural basis of human KCNQ1 modulation and gating. *Cell* **180**, 340–347.e9 (2020).
23. M. A. Zaydman *et al.*, Kv7.1 ion channels require a lipid to couple voltage sensing to pore opening. *Proc. Natl. Acad. Sci. U.S.A.* **110**, 13180–13185 (2013).
24. F. Yang *et al.*, Structural mechanism underlying capsaicin binding and activation of the TRPV1 ion channel. *Nat. Chem. Biol.* **11**, 518–524 (2015).
25. A. Kamb, L. E. Iverson, M. A. Tanouye, Molecular characterization of Shaker, a *Drosophila* gene that encodes a potassium channel. *Cell* **50**, 405–413 (1987).
26. T. Hoshi, W. N. Zagotta, R. W. Aldrich, Biophysical and molecular mechanisms of Shaker potassium channel inactivation. *Science* **250**, 533–538 (1990).
27. N. E. Ottosson, S. I. Liin, F. Elinder, Drug-induced ion channel opening tuned by the voltage sensor charge profile. *J. Gen. Physiol.* **143**, 173–182 (2014).
28. S. I. Liin, U. Karlsson, B. H. Bentzen, N. Schmitt, F. Elinder, Polyunsaturated fatty acids are potent openers of human M-channels expressed in *Xenopus laevis* oocytes. *Acta Physiol. (Oxf.)* **218**, 28–37 (2016).
29. M. Silverå Ejneby *et al.*, Atom-by-atom tuning of the electrostatic potassium-channel modulator dehydroabietic acid. *J. Gen. Physiol.* **150**, 731–750 (2018).
30. N. E. Ottosson *et al.*, Resin-acid derivatives as potent electrostatic openers of voltage-gated K channels and suppressors of neuronal excitability. *Sci. Rep.* **5**, 13278 (2015).
31. S. I. Börjesson, T. Parkkari, S. Hammarström, F. Elinder, Electrostatic tuning of cellular excitability. *Biophys. J.* **98**, 396–403 (2010).
32. S. I. Börjesson, S. Hammarström, F. Elinder, Lipoelectric modification of ion channel voltage gating by polyunsaturated fatty acids. *Biophys. J.* **95**, 2242–2253 (2008).